X-Ray Properties of Young Stars and Stellar Clusters

Eric Feigelson and Leisa Townsley
Pennsylvania State University

Manuel Güdel
Paul Scherrer Institute

Keivan Stassun
Vanderbilt University

Although the environments of star and planet formation are thermodynamically cold, substantial X-ray emission from 10–100 MK plasmas is present. In low-mass pre-main-sequence stars, X-rays are produced by violent magnetic reconnection flares. In high-mass O stars, they are produced by wind shocks on both stellar and parsec scales. The recent Chandra Orion Ultradeep Project, XMM-Newton Extended Survey of Taurus, and Chandra studies of more distant high-mass star-forming regions reveal a wealth of X-ray phenomenology and astrophysics. X-ray flares mostly resemble solar-like magnetic activity from multipolar surface fields, although extreme flares may arise in field lines extending to the protoplanetary disk. Accretion plays a secondary role. Fluorescent iron line emission and absorption in inclined disks demonstrate that X-rays can efficiently illuminate disk material. The consequent ionization of disk gas and irradiation of disk solids addresses a variety of important astrophysical issues of disk dynamics, planet formation, and meteoritics. New observations of massive star-forming environments such as M 17, the Carina Nebula, and 30 Doradus show remarkably complex X-ray morphologies including the low-mass stellar population, diffuse X-ray flows from blister HII regions, and inhomogeneous superbubbles. X-ray astronomy is thus providing qualitatively new insights into star and planet formation.

1. INTRODUCTION

Star and planet formation is generally viewed as a hydrodynamic process involving gravitational collapse of interstellar material at low temperatures, 10–100 K in molecular cloud cores and 100–1500 K in protoplanetary disks. If thermodynamical equilibrium holds, this material should be neutral except in localized HII regions where the bolometric ultraviolet emission from massive O-star photoionization is present. However, stars have turned out to be sources of intense X-rays at almost every stage of early formation and evolution, from low-mass brown dwarfs to massive O stars, to an extent that the stellar environment is ionized and heated (beyond effects due to ultraviolet radiation) out to considerable distances and thus made accessible to magnetic fields.

X-ray observations reveal the presence of highly ionized plasma with temperatures of 10^7–10^8 K. In lower-mass stars, the X-ray emission is reminiscent of X-rays observed on the Sun, particularly the plasma explosively heated and confined in magnetic loops following magnetic reconnection events. X-ray flares with luminosities orders of magnitude more powerful than seen in the contemporary Sun are frequently seen in young stars. Evidence for an impulsive phase is seen in radio bursts and in U-band enhancements preceding X-ray flares, thought to be due to the bombardment of the stellar surface by electron beams. Thus, young stars prolifically accelerate particles to relativistic energies. In rich young stellar clusters, X-rays are also produced by shocks in O-star winds, on both small ($<10^2$ $R_\star$) and large (parsec) scales. If the region has been producing rich clusters for a sufficiently long time, the resulting supernova remnants will dominate the X-ray properties.

X-ray studies with the Chandra and XMM-Newton space observatories are propelling advances of our knowledge and understanding of high-energy processes during the earliest phases of stellar evolution. In the nearest young stars and clusters ($d < 500$ pc), they provide detailed information about magnetic reconnection processes. In the more distant and richer regions, the X-ray images are amazingly complex with diffuse plasma surrounding hundreds of stars exhibiting a wide range of absorptions. We concentrate here on results from three recent large surveys: the Chandra Orion Ultradeep Project (COUP), based on a nearly continuous 13-day observation of the Orion Nebula region in 2003; the XMM-Newton Extended Survey of Taurus (XEST) that maps ~5 deg^2 of the Taurus Molecular Cloud (TMC); and an ongoing Chandra survey of high-mass star-formation regions across the galactic disk. Because the XEST study is discussed in specific detail in a closely related chapter (see chapter by Güdel et al.) together with optical and infrared surveys, we present only selected XEST results. This vol-

ume has another closely related chapter: Bally et al. discuss X-ray emission from high-velocity protostellar Herbig-Haro outflows. The reader interested in earlier X-ray studies is referred to reviews by *Feigelson and Montmerle* (1999), *Glassgold et al.* (2000), *Favata and Micela* (2003), *Paerels and Kahn* (2003), and *Güdel* (2004).

The COUP is particularly valuable in establishing a comprehensive observational basis for describing the physical characteristics of flaring phenomena and elucidating the mechanisms of X-ray production. The central portion of the COUP image, showing the PMS population around the bright Trapezium stars and the embedded OMC-1 populations, is shown in Plate 1 (*Getman et al.,* 2005a). X-rays are detected from nearly all known optical members except for many of the bolometrically fainter M stars and brown dwarfs. Conversely, 1315 of 1616 COUP sources (81%) have clear cluster member counterparts and ≃75 (5%) are new obscured cloud members; most of the remaining X-ray sources are extragalactic background sources seen through the cloud (*Getman et al.,* 2005b).

X-ray emission and flaring is thus ubiquitous in PMS stars across the initial mass function (IMF). The X-ray luminosity function (XLF) is broad, spanning $28 < \log L_x[\mathrm{erg/s}] < 32$ (0.5–8 keV), with a peak around $\log L_x[\mathrm{erg/s}] \sim 29$ (*Feigelson et al.,* 2005). For comparison, the contemporary Sun emits $26 < \log L_x[\mathrm{erg/s}] < 27$, with flares up to 10^{28} erg/s, in the same spectral band. Results from the more distributed star formation clouds surveyed by XEST reveal a very similar X-ray population as in the rich cluster of the Orion Nebula, although confined to stars with masses mostly below 2 $M_\odot$ (see chapter by Güdel et al.), although there is some evidence the XLF is not identical in all regions (section 4.1). There is no evidence for an X-ray-quiet, nonflaring PMS population.

The empirical findings generate discussion on a variety of astrophysical implications, including the nature of magnetic fields in young stellar systems, the role of accretion in X-ray emission, the effects of X-ray irradiation of protoplanetary disks and molecular clouds, and the discovery of X-ray flows from HII regions. A number of important related issues are not discussed here, including discovery of heavily obscured X-ray populations, X-ray identification of older PMS stars, the X-ray emission of intermediate mass Herbig Ae/Be stars, the enigmatic X-ray spectra of some O stars, the generation of superbubbles by OB clusters and their multiple supernova remnants, and the large scale starburst conditions in the galactic center region and other galactic nuclei.

2. FLARING IN PRE-MAIN-SEQUENCE STARS

2.1. The Solar Model

Many lines of evidence link the PMS X-ray properties to magnetic activity on the Sun and other late-type magnetically active stars such as dMe flare stars, spotted BY Dra variables, and tidally spun-up RS CVn post-main-sequence binaries. These systems have geometrically complex multipolar magnetic fields in arcades of loops rooted in the stellar photospheres and extending into the coronae. The field lines become twisted and tangled by gas convection and undergo explosive magnetic reconnection. The reconnection immediately accelerates a population of particles with energies tens of keV to several MeV; this is the "impulsive phase" manifested by gyrosynchrotron radio continuum emission, blue optical/UV continuum, and, in the Sun, high γ-ray and energetic particle fluences. These particles impact the stellar surface at the magnetic footprints, immediately heating gas that flows upward to fill coronal loops with X-ray emitting plasma. It is this "gradual phase" of the flare that is seen with X-ray telescopes. *Schrijver and Zwaan* (2000) and *Priest and Forbes* (2002) review the observations and physics of solar and stellar flares.

Extensive multiwavelength properties of PMS stars indicate they are highly magnetically active stars (*Feigelson and Montmerle,* 1999). Hundreds of Orion stars, and many in other young stellar populations, have periodic photometric variations from rotationally modulated starspots covering 10–50% of the surface (*Herbst et al.,* 2002). A few of these have been subject to detailed Doppler mapping showing spot structure. Radio gyrosynchrotron emission from flare electrons spiraling in magnetic loops has been detected in several dozen PMS stars (*Güdel,* 2002). A few nearby PMS stars have Zeeman measurements indicating that kiloGauss fields cover much of the surface (*Johns-Krull et al.,* 2004). In the COUP and XEST studies, temperatures inferred from time-averaged spectra extends the T_{cool}–T_{hot} and T–L_x trends found in the Sun and older stars to higher levels (*Preibisch et al.,* 2005; Telleschi et al., in preparation). X-ray spectra also show plasma abundance anomalies that are virtually identical to those seen in older magnetically active stars (*Scelsi et al.,* 2005; Maggio et al., in preparation).

Taking advantage of the unprecedented length of the COUP observation, *Flaccomio et al.* (2005) find rotational modulation of X-ray emission in at least 10% of Orion PMS stars with previously determined rotation periods from optical monitoring. An example is shown in Fig. 1a. Amplitudes of variability range from 20% to 70% and X-ray periods generally agree with the optical periods. In a few cases, it is half the optical value, implying X-ray-emitting regions on opposite hemispheres. This result indicates that in at least some PMS stars, the X-rays are emitting from relatively long-lived structures lying low in the corona that are inhomogeneously distributed around the star. Similar X-ray rotational modulations are seen in the Sun and a few older stars.

Wolk et al. (2005) examined the flaring behavior of a complete sample of solar analogs ($0.9 < M/M_\odot < 1.2$) in the Orion Nebula Cluster. The lightcurve in Fig. 1b shows one of the more spectacular flares in this subsample reaching $\log L_x(\mathrm{peak})[\mathrm{erg/s}] = 32.2$. Most flares show solar-type rapid rise and slower decay; the decay phase can last from <1 h to >3 d. The brightness and spectral variations during the decay phases of this and similarly powerful Orion flares have been analyzed by *Favata et al.* (2005a) using a loop

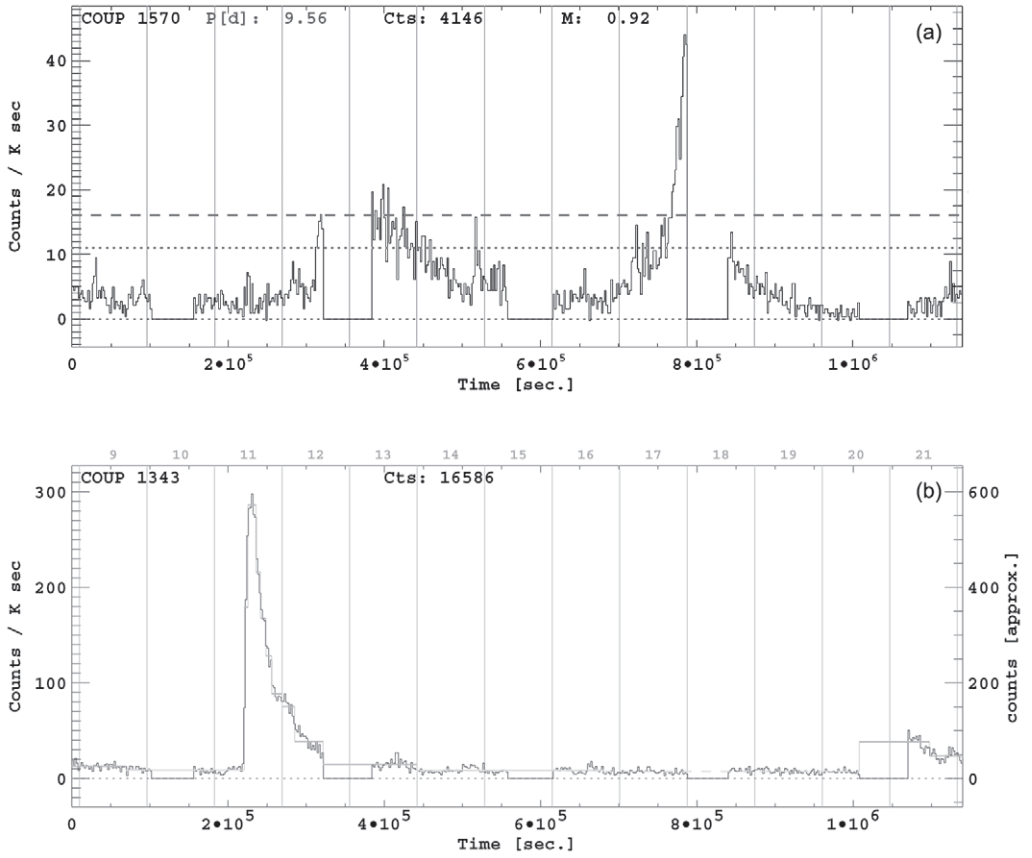

Fig. 1. Two of 1400+ X-ray lightcurves from the Chandra Orion Ultradeep Project. The abscissa is time spanning 13.2 d, and the ordinate gives X-ray count rate in the 0.5–8 keV band. **(a)** An Orion star showing typical PMS flaring behavior superposed on a rotational modulation of the "characteristic" emission. From *Flaccomio et al.* (2005). **(b)** COUP #1343 = JW 793, a poorly characterized PMS star in the Orion Nebula, showing a spectacular solar-type flare. From *Wolk et al.* (2005) and *Favata et al.* (2005a).

model previously applied to "gradual" (i.e., powerful events spanning several hours) solar and stellar flares. The result for COUP #1343 and other morphologically simple cases is clear: The drop in X-ray emission and plasma temperature seen in PMS stellar flares is completely compatible with that of older stars. In some COUP flares, the decay shows evidence of continued or episodic reheating after the flare peak, a phenomenon also seen in solar flares and in older stars.

The intensity of PMS flaring is remarkably high. In the solar analog sample, flares brighter than $L_x(\text{peak}) \geq 2 \times 10^{30}$ erg/s occur roughly once a week (*Wolk et al.,* 2005). The most powerful flares have peak luminosities up to several times 10^{32} erg/s (*Favata et al.,* 2005a). The peak plasma temperature are typically T (peak) ≃ 100 MK but sometimes appear much higher. The time-integrated energy emitted in the X-ray band during flares in solar-mass COUP stars is $\log E_x[\text{erg}] \simeq 34$–$36$. An even more remarkable flare with $\log E_x[\text{erg}] \simeq 37$ was seen by ROSAT from the nonaccreting Orion star Parenago 1724 in 1992 (*Preibisch et al.,* 1995). These values are far above solar flaring levels: The COUP flares are $10^2\times$ stronger and $10^2\times$ more frequent than the most powerful flares seen in the contemporary Sun; the implied fluence of energetic particles may be $10^5\times$ above solar levels (*Feigelson et al.,* 2002).

The Orion solar analogs emit a relatively constant "characteristic" X-ray level about three-fourths of the time (see Fig. 1). The X-ray spectrum of this characteristic state can be modeled as a two-temperature plasma with one component $T_{\text{cool}} \simeq 10$ MK and the other component $T_{\text{hot}} \simeq 30$ MK. These temperatures are much higher than the quiescent solar corona. The concept of "microflaring" or "nanoflaring" for the Sun has been widely discussed (*Parker,* 1988) and has gained favor in studies of older magnetically active stars based on lightcurve and spectral analysis (*Kashyap et al.,* 2002; *Güdel et al.,* 2003, *Arzner and Güdel,* 2004). These latter studies of dMe flare stars indicate that a power-law distribution of flare energies, $dN/dE \propto E^{-\alpha}$, is present with $\alpha \simeq 2.0$–2.7. The energetics is clearly dominated by smaller flares. The COUP lightcurves vary widely in appearance, but collectively can also be roughly simulated by a power law with $\alpha \simeq 2.0$–2.5 without a truly quiescent component (*Flaccomio et al.,* 2005). Thus, when reference is made to the more easily studied superflares, one must always re-

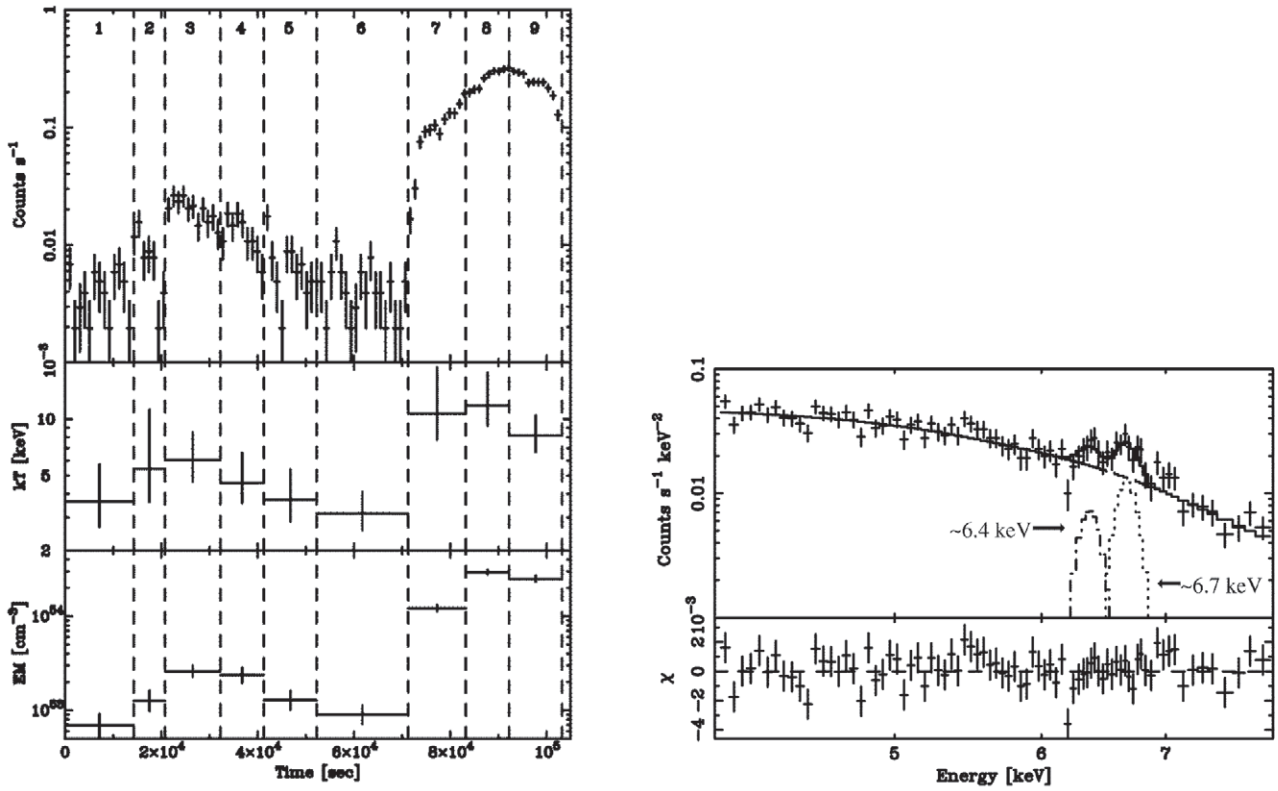

Fig. 2. X-ray flare from Class I protostar YLW 16A in the ρ Ophiuchi cloud, observed with Chandra. The flare has an unusual morphology and the spectrum shows very hot plasma temperatures with strong emission from the fluorescent 6.4 keV line of neutral iron attributable to reflection off the protoplanetary disk. From *Imanishi et al.* (2001).

member that many more weaker flares are present and may have comparable or greater astrophysical effects. Not infrequently, secondary flares and reheating events are seen superposed on the decay phase of powerful flares (e.g., *Gagné et al.,* 2004; *Favata et al.,* 2005a).

One puzzle with a solar model for PMS flares is that some show unusually slow rises. The nonaccreting star LkHα 312 exhibited a 2-h fast rise with peak temperature T ≃ 88 MK, followed by a 6-h slower rise to log L_x(peak) [erg/s] = 32.0 (*Grosso et al.,* 2004). The flare from the Class I protostar YLW 16A in the dense core of the ρ Ophiuchi cloud showed a remarkable morphology with two rise phases and similar temperature structure (Fig. 2) (*Imanishi et al.,* 2001). Other flares seen with COUP show roughly symmetrical rise and fall morphologies, sometimes extending over 1–2 days (*Wolk et al.,* 2005). It is possible that some of these variations are due to the stellar rotation where X-ray structures are emerging from eclipse, but they are currently poorly understood.

By monitoring young stars with optical telescopes simultaneous with X-ray observations, the early impulsive phase of PMS flares can be revealed. This has been achieved with distributed groundbased telescopes and in space: The XMM-Newton satellite has an optical-band telescope coaligned with the X-ray telescope. During the impulsive phase, electron beams accelerated after the reconnection event bombard the stellar chromosphere, which produces a burst of short-wavelength optical and UV radiation. XMM-Newton observation of the Taurus PMS star GK Tau shows both uncorrelated modulations as well as a strong U-band burst preceding an X-ray flare in good analogy with solar events (Audard et al., in preparation) (Fig. 3a). Groundbased optical and Hα monitoring of the Orion Nebula during the COUP campaign revealed one case of an I-band spike simultaneous with a very short X-ray flare of intermediate brightness (*Stassun et al.,* 2006) (Fig. 3b).

2.2. The Role of Accretion

It was established in the 1980s and 1990s that elevated levels of X-ray emission in PMS stars appears in both "classical" T Tauri stars, with optical/infrared signatures of accretion from a protoplanetary disk, and "weak-lined" T Tauri stars, without these signatures. This basic result is confirmed but with some important refinements — and controversy — from recent studies.

While the presence or absence of a K-band emitting inner disk does not appear to influence X-ray emission, the presence of accretion has a *negative* impact on X-ray production (*Flaccomio et al.,* 2003; *Stassun et al.,* 2004; *Preibisch et al.,* 2005; Telleschi et al., in preparation). This is manifested as a statistical decrease in X-rays by a factor of

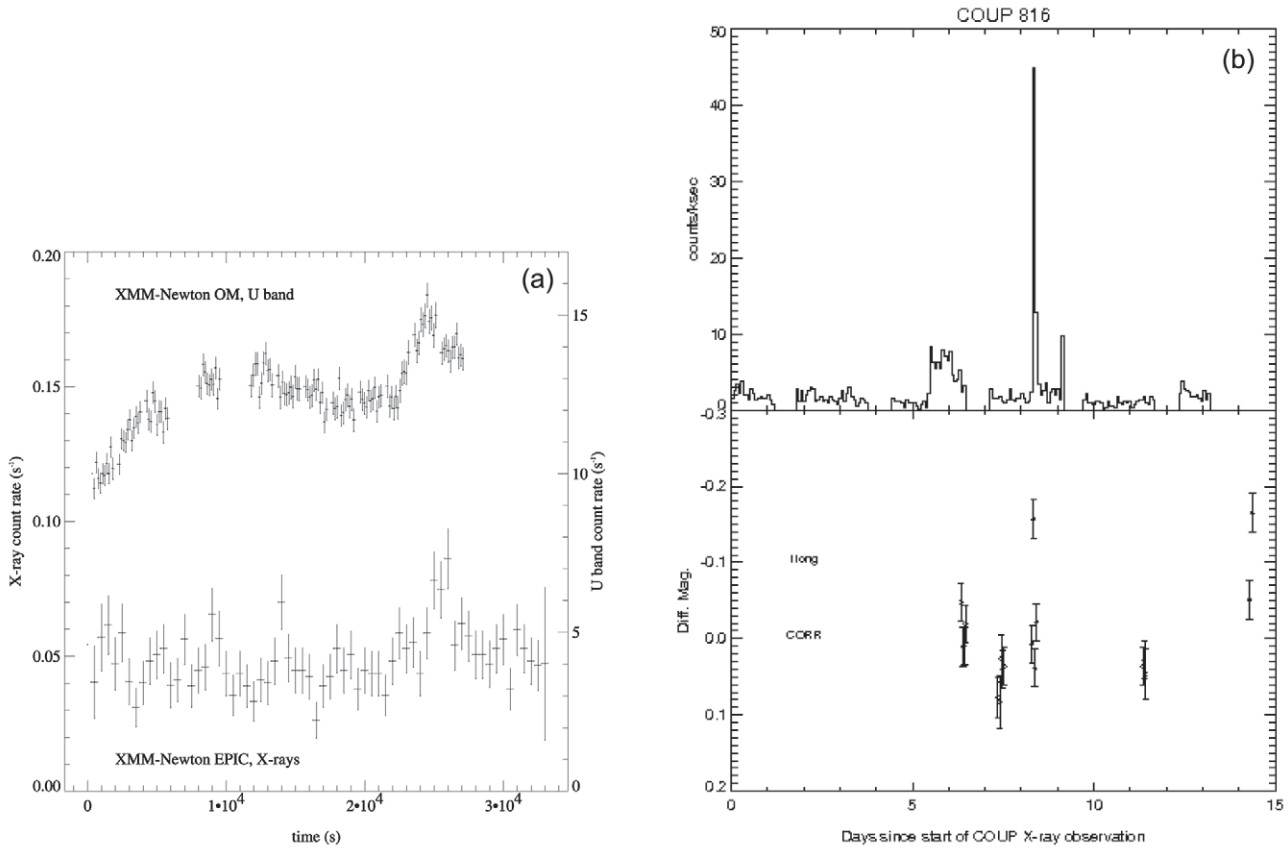

Fig. 3. Detection of the "white light" component during the impulsive phases of PMS X-ray flares. **(a)** Short-term behavior of the classical T Tau binary GK Tau in U-band light (upper curve) and X-rays (lower curve) from the XEST survey. The lightcurve covers approximately 9 h. From Audard et al. (in preparation). **(b)** Rapid X-ray flare (top panel) from COUP #816 = JW 522, an obscured PMS star in the Orion Nebula Cluster, apparently accompanied by impulsive I-band emission. This COUP X-ray lightcurve spans 13.2 d. From *Stassun et al.* (2006).

2–3 in accreting vs. nonaccreting PMS stars, even after dependencies on mass and age are taken into account. The effect does not appear to arise from absorption by accreting gas; e.g., the offset appears in the hard 2–8-keV band where absorption is negligible. The offset is relatively small compared to the 10^4 range in the PMS X-ray luminosity function, and flaring behavior is not affected in any obvious way. One possible explanation is that mass-loaded accreting field lines cannot emit X-rays (*Preibisch et al.,* 2005). If a magnetic reconnection event liberates a certain amount of energy, this energy would heat the low-density plasma of nonaccretors to X-ray emitting temperatures, while the denser plasma in the mass-loaded magnetic field lines would be heated to much lower temperatures. The remaining field lines that are not linked to the disk would have low coronal densities and continue to produce solar-like flares. Note that the very young accreting star XZ Tau shows unusual temporal variations in X-ray absorption that can be attributed to eclipses by the accretion stream (*Favata et al.,* 2003).

The optical observations conducted simultaneously with the COUP X-ray observations give conclusive evidence that accretion does not produce or suppress flaring in the great majority of PMS stars (*Stassun et al.,* 2006). Of the 278 Orion stars exhibiting variations in both optical and X-ray bands, not a single case is found where optical variations (attributable to either rotationally modulated starspots or to changes in accretion) have an evident effect on the X-ray flaring or characteristic emission.

An example from the XEST survey is shown in Fig. 3a where the slow modulation seen in the first half is too rapid for effects due to rotation, but on the other hand shows no equivalent signatures in X-rays. The optical fluctuations are therefore unrelated to flare processes and, in this case, are likely due to variable accretion (Audard et al., in preparation). Similarly, a Taurus brown dwarf with no X-ray emission detected in XEST showed a slow rise by a factor of 6 over eight hours in the U-band flux (*Grosso et al.,* 2006). Such behavior is uncommon for a flare, and because this brown dwarf is accreting, mass streams may again be responsible for producing the excess ultraviolet flux.

The simplest interpretation of the absence of statistical links between accretion and X-ray luminosities and the absence of simultaneous optical/X-ray variability is that different magnetic field lines are involved with funneling gas

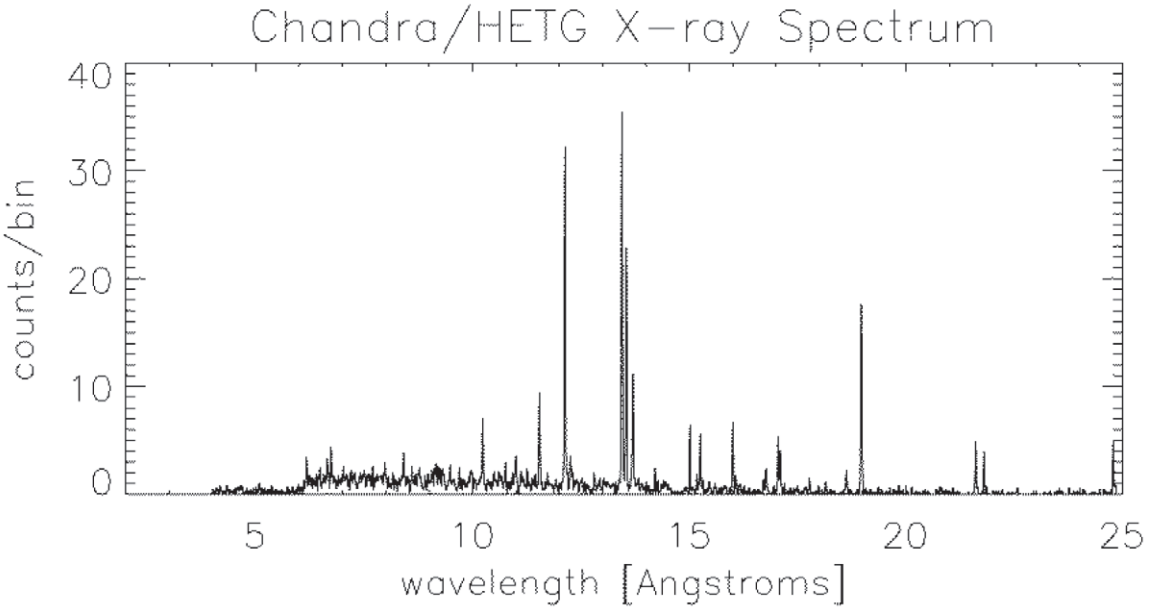

Fig. 4. High-resolution transmission grating spectrum of the nearest classical T Tauri star, TW Hya. The spectrum is softer than other PMS stars, and the triplet line ratios imply either X-ray production in a high-density accretion shock or irradiation by ultraviolet radiation. From *Kastner et al.* (2002).

from the disk and with reconnection events producing X-ray plasma. There is no evidence that the expected shock at the base of the accretion column produces the X-rays seen in COUP and XEST.

There are some counterindications to these conclusions. A huge increase in X-ray emission was seen on long timescales from the star illuminating McNeil's Nebula, which exhibited an optical/infrared outburst attributed to the onset of rapid accretion (*Kastner et al.,* 2004). In contrast, however, X-rays are seen before, during, and after outburst of the EXor star V1118 Ori, with a lower temperature seen when accretion was strongest (*Audard et al.,* 2005). These findings suggest that accretion, and perhaps the inner disk structure, might sometimes affect magnetic field configurations and flaring in complicated ways.

The biggest challenge comes from TW Hya, the nearest and brightest accreting PMS star. It has an X-ray spectrum much softer than most COUP or other PMS sources (Fig. 4). Due to its proximity to the Sun, TW Hya is sufficiently bright in X-rays to be subject to detailed high-resolution spectroscopy using transmission gratings on the Chandra and XMM-Newton telescopes (*Kastner et al.,* 2002; *Stelzer and Schmitt,* 2004; *Ness and Schmitt,* 2005). According to the magnetospheric accretion scenario, accreted material crashes onto the stellar surface with velocities of up to several hundred km/s, which should cause ~10^6 K shocks in which strong optical and UV excess emission and perhaps also soft X-ray emission is produced (*Lamzin,* 1999). Density-sensitive triplet line ratios of Ne IX and O VII are saturated, indicating either that the emitting plasma has densities log n_e[cm^{-3}] ~ 13, considerably higher than the log n_e[cm^{-3}] ~ 10 characteristic of low-level coronal emission although reminiscent of densities in flares. However, these densities were measured during an observation dominated by relative quiescence with no hot plasma present. Alternatively, the high triplet ratios might be induced by plasma subject to strong ultraviolet irradiation. A similar weak forbidden line in the O VII triplet is seen in the accreting PMS star BP Tau (*Schmitt et al.,* 2005), and similar soft X-ray emission is seen from the Herbig Ae star HD 163296 (*Swartz et al.,* 2005).

If the plasma material in TW Hya is drawn from the disk rather than the stellar surface, one must explain the observed high Ne/Fe abundance ratio that is similar to that seen in flare plasmas. One possibility is that the abundance anomalies do not arise from the coronal first ionization potential effect, but rather from the depletion of refractory elements into disk solids (*Brinkman et al.,* 2001; *Drake et al.,* 2005). This model, however, must confront models of the infrared disk indicating that grains have sublimated in the disk around 4 AU, returning refractory elements back into the gas phase (*Calvet et al.,* 2002).

Finally, we note that current X-ray instrumentation used for PMS imaging studies is not very sensitive to the cooler plasma expected from accretion shocks, and that much of this emission may be attenuated by line-of-sight interstellar material. The possibility that some soft accretion X-ray emission is present in addition to the hard flare emission is difficult to firmly exclude. But there is little doubt that most of the X-rays seen with Chandra and XMM-Newton are generated by magnetic reconnection flaring rather than the accretion process.

2.3. The Role of Disks

There are strong reasons from theoretical models to believe that PMS stars are magnetically coupled to their disks at the corotation radii typically 5–10 $R_\star$ from the stellar surface (e.g., *Hartmann,* 1998; *Shu et al.,* 2000). This hypothesis unifies such diverse phenomena as the self-absorbed optical emission lines, the slow rotation of accreting PMS stars, and the magnetocentrifugal acceleration of Herbig-Haro jets. However, there is little *direct* evidence for magnetic field lines connecting the star and the disk. Direct imaging of large-scale magnetic fields in PMS stars is only possible today using very long baseline interferometry at radio wavelengths where an angular resolution of 1 mas corresponds to 0.14 AU at the distance of the Taurus or Ophiuchus clouds. But only a few PMS stars are sufficiently bright in radio continuum for such study. One of the components of T Tau S has consistently shown evidence of magnetic field extensions to several stellar radii, perhaps connecting to the inner border of the accretion disk (*Loinard et al.,* 2005).

But X-ray flares can provide supporting evidence for star-disk magnetic coupling. An early report of star-disk fields arose from a sequence of three powerful flares with separations of ~20 h from the Class I protostar YLW 15 in the ρ Oph cloud (*Tsuboi et al.,* 2000). Standard flare plasma models indicated loop lengths around 14 $R_\odot$, and periodicity might arise from incomplete rotational star-disk coupling (*Montmerle et al.,* 2000). However, it is also possible that the YLA 15 flaring is not truly periodic; many cases of multiple flares without periodicities are seen in the COUP lightcurves.

Analysis of the most luminous X-ray flares in the COUP study also indicates that huge magnetic structures can be present. *Favata et al.* (2005a) reports analysis of the flare decay phases in sources such as COUP #1343 (Fig. 1) using models that account for reheating processes, which otherwise can lead to overestimation of loop lengths. The combination of very high luminosities ($\log L_X$(peak)[erg/s] ≃ 31–32), peak temperatures in excess of 100 MK, and very slow decays appear to require loops much larger than the star, up to several 10^{12} cm or 5–20 $R_\star$. Recall that these flares represent only the strongest ~1% of all flares observed by COUP; most flares from PMS stars are much weaker and likely arise from smaller loops. This is clearly shown in some stars by the rotational modulation of the nonflaring component in the COUP study (*Flaccomio et al.,* 2005).

Given the typical 2–10-d rotation periods of PMS stars, is seems very doubtful such long flaring loops would be stable if both footpoints were anchored to the photosphere. Even if MHD instabilities are not important, gas pressure and centrifugal forces from the embedded plasma may be sufficient to destroy such enormous coronal loops (*Jardine and Unruh,* 1999). *Jardine et al.* (2006) develop a model of magnetically confined multipolar coronae of PMS stars where accretion follows some field lines while others contain X-ray emitting plasma; the model also accounts for observed statistical relations between X-ray properties and stellar mass.

The magnetospheres of PMS stars are thus likely to be quite complex. Unlike the Sun where only a tiny fraction of the photosphere has active regions, intense multipolar fields cover much of the surface in extremely young stars. Continuous microflaring is likely responsible for the ubiquitous strong 10–30-MK plasma emission. Other field lines extend several stellar radii: Some are mass-loaded with gas accreting from the circumstellar disk, while others may undergo reconnection producing the most X-ray-luminous flares.

3. THE EVOLUTION OF MAGNETIC ACTIVITY

The COUP observation provides the most sensitive, uniform, and complete study of X-ray properties for a PMS stellar population available to date. When combined with studies of older stellar clusters, such as the Pleiades and Hyades, and of volume-limited samples in the solar neighborhood, evolutionary trends in X-ray emission can be traced. Since chromospheric indicators of magnetic activity (such as Ca II line emission) are confused by accretion, and photospheric variations from rotationally modulated starspots are too faint to be generally measured in most older stars, X-ray emission is the only magnetic indicator that can be traced in stellar populations from 10^5 to 10^{10} yr. The result from the PMS to the giga-year-old disk population is shown in Fig. 5a (*Preibisch and Feigelson,* 2005). The two critical advantages here over other measures of magnetic activity evolution are the complete samples (and correct treatment of nondetections) and stratification by mass. The latter is important because the mass-dependence of X-ray luminosities (for unknown reasons) differs in PMS and main-sequence stars (*Preibisch et al.,* 2005).

If one approximates the decay of magnetic activity as a power law, then evolution in the $0.5 < M < 1.2\ M_\odot$ mass range is approximately power-law with $L_X \propto \tau^{-3/4}$ over the wide range of ages $5 < \log \tau\ [\mathrm{yr}] < 9.5$. Other X-ray studies of older disk stars suggest that the decay rate steepens: $L_X \propto \tau^{-3/2}$ or τ^{-2} over $8 < \log \tau\ [\mathrm{yr}] < 10$ (*Güdel et al.,* 1997; *Feigelson et al.,* 2004). Note, however, that *Pace and Pasquini* (2004) find no decay in chromospheric activity in a sample of solar mass stars after 3 G.y. These results are similar to, but show more rapid decay than, the classical *Skumanich* (1972) $\tau^{-1/2}$ relation that had been measured for main-sequence stars only over the limited age range $7.5 < \log \tau\ [\mathrm{yr}] < 9.5$. The COUP sample also exhibits a mild decay in magnetic activity for ages $5 < \log \tau\ [\mathrm{yr}] < 7$ within the PMS phase, although the trend is dominated by star-to-star scatter (*Preibisch and Feigelson,* 2005).

While these results would appear to confirm and elaborate the long-standing rotation-age-activity relationship of solar-type stars, the data paint a more complex picture. The Chandra Orion studies show that the rotation-activity relation is largely absent at 1 m.y. (*Stassun et al.,* 2004; *Preibisch et al.,* 2005). This finding suggests the somewhat

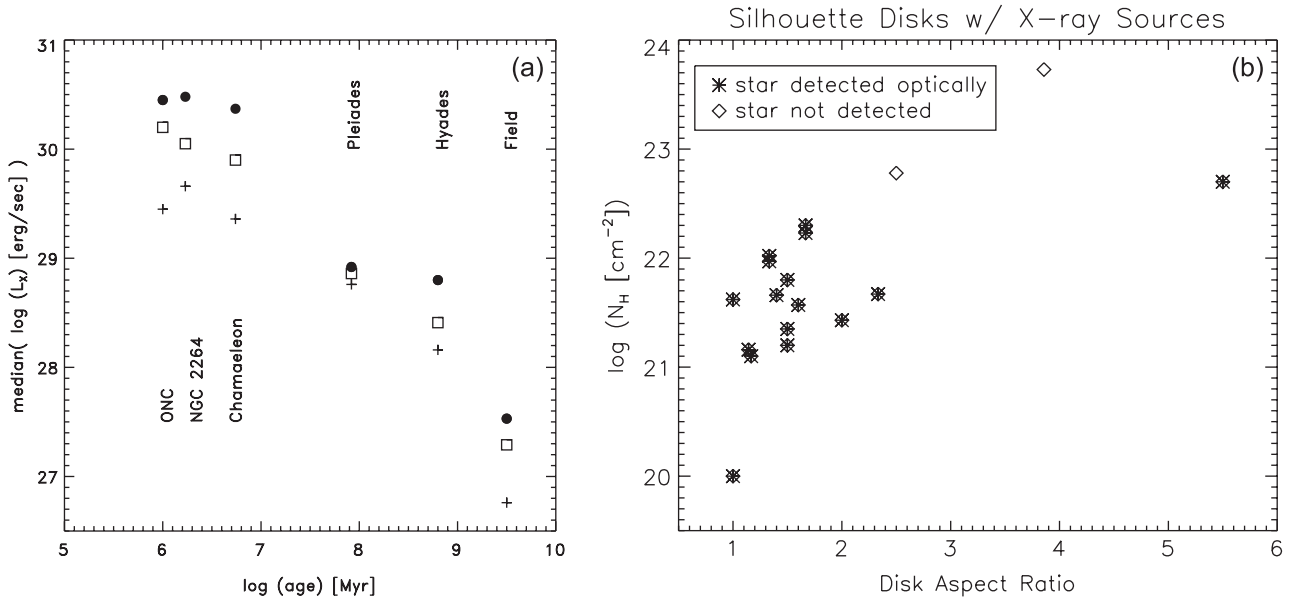

Fig. 5. **(a)** Evolution of the median X-ray luminosities for stars in different mass ranges: 0.9–1.2 $M_\odot$ (solid circles), 0.5–0.9 $M_\odot$ (open squares), and 0.1–0.5 $M_\odot$ (plusses). From *Preibisch and Feigelson* (2005). **(b)** The link between soft X-ray absorption and proplyd inclination is the first measurement of gas column densities in irradiated disks. From *Kastner et al.* (2005).

surprising result that the activity-age decay is strong across the entire history of solar-type stars but is not entirely attributable to rotational deceleration. The PMS magnetic fields may either be generated by a solar-type dynamo that is completely saturated, or by a qualitatively different dynamo powered by turbulence distributed throughout the convective interior rather than by rotational shear at the tachocline. At the same time, the Orion studies show a small *positive* correlation between rotation period and X-ray activity, similar to that seen in the "supersaturated" regime of main-sequence stars. It is also possible that this effect is due to a sample bias against slowly rotating, X-ray-weak Orion stars (*Stassun et al.,* 2004).

The XEST findings in the Taurus PMS population give a different result, suggesting that an unsaturated solar-type dynamo may in fact be present in PMS stars when rotation periods are longer than a few days (Briggs et al., in preparation). It is possible that the somewhat more evolved Taurus sample, compared to the Orion Nebula Cluster stars, has produced sufficiently prominent radiative zones in some of these late-type PMS stars to put a solar-type dynamo into operation.

The origins of magnetic fields in PMS stars are thus still not well established. It is possible that both tachoclinal and convective dynamos are involved, as discussed by *Barnes* (2003a,b). There is a hint of a transition between convective and rotational dynamos in the plot of L_x/L_{bol} against mass in Orion stars. The X-ray emissivity for many stars drops precipitously for masses above 2–3 $M_\odot$, which is also the boundary between lower-mass convective and higher-mass radiative interiors (*Feigelson et al.,* 2003). Another possible influence is that accretion in younger PMS stars alters convection and thereby influences the magnetic field generation process (*Siess et al.,* 1999; *Stassun et al.,* 2004).

The magnetic activity history for M stars with masses 0.1–0.4 $M_\odot$ appears to be different than more massive PMS stars (Fig. 5a). Only a mild decrease in X-ray luminosity, and even a mild increase in L_x/L_{bol}, is seen over the $6 < \log \tau$ [yr] < 8 range, though the X-ray emission does decay over giga-year timescales. This result may be related to the well-established fact that the low-mass M stars have much longer rotational slow-down times than solar-type stars. But the difference in behavior compared to higher-mass stars could support the idea that the dynamos in PMS and dM stars both arise from a convective turbulent dynamo. These issues are further discussed in *Mullan and MacDonald* (2001), *Feigelson et al.* (2003), *Barnes* (2003a), and *Preibisch et al.* (2005).

An unresolved debate has emerged concerning the onset of X-ray emission in PMS stars. There is no question that magnetic activity with violent flaring is common among Class I protostars with ages ~10^5 yr (*Imanishi et al.,* 2001; *Preibisch,* 2004) (Fig. 2). The question is whether X-ray emission is present in Class 0 protostars with ages ~10^4 yr. There is one report of hard X-rays from two Class 0 protostars in the OMC 2/3 region (*Tsuboi et al.,* 2001); however, other researchers classify the systems as Class I (*Nielbock et al.,* 2003). An X-ray emitting protostar deeply embedded in the R Corona Australis cloud core has a similarly uncertain Class 0 or I status (*Hamaguchi et al.,* 2005). In contrast, a considerable number of well-established Class 0 protostars appear in Chandra images and are not detected;

e.g., in the NGC 1333 and Serpens embedded clusters (*Getman et al.,* 2002; *Preibisch,* 2004). However, because Class 0 stars are typically surrounded by very dense gaseous envelopes, it is possible that the X-ray nondetections arise from absorption rather than an absence of emission. An interesting new case is an intermediate-mass Class 0 system in the IC 1396N region that exhibits extremely strong soft X-ray absorption (*Getman et al.,* 2006b).

4. X-RAY STARS AND HOT GAS IN MASSIVE STAR-FORMING REGIONS

Most stars are born in massive star-forming regions (MSFRs) where rich clusters containing thousands of stars are produced in molecular cloud cores. Yet, surprisingly little is known about the lower mass populations of these rich clusters. Beyond the Orion Molecular Clouds, near-infrared surveys like 2MASS are dominated by foreground or background stars, and the initial mass functions are typically measured statistically rather than by identification of individual cluster members. X-ray surveys of MSFRs are important in this respect because they readily discriminate young stars from unrelated objects that often contaminate JHK images of such fields, especially for those young stars no longer surrounded by a dusty circumstellar disk. Furthermore, modern X-ray telescopes penetrate heavy obscuration (routinely $A_V \sim 10$–100 mag, occasionally up to 1000 mag) with little source confusion or contamination from unrelated objects to reveal the young stellar populations in MSFRs.

The O and Wolf-Rayet (WR) members of MSFRs have been catalogued, and the extent of their UV ionization is known through HII region studies. But often little is known about the fate of their powerful winds. The kinetic power of a massive O star's winds injected into its stellar neighborhood over its lifetime is comparable to the input of its supernova explosion. Theorists calculate that wind-blown bubbles of coronal-temperature gas should be present, but no clear measurement of this diffuse plasma had been made in HII regions prior to Chandra. X-ray studies also detect the presence of earlier generations of OB stars through the shocks of their supernova remnants (SNRs). In very rich and long-lived star-forming cloud complexes, SNRs combine with massive stellar winds to form superbubbles and chimneys extending over hundreds of parsecs and often into the galactic halo. O stars are thus the principal drivers of the interstellar medium.

The MSFR X-ray investigations discussed here represent only a fraction of this rapidly growing field. A dozen early observations of MSFRs by Chandra and XMM-Newton are summarized by *Townsley et al.* (2003). Since then, Chandra has performed observations of many other regions, typically revealing hundreds of low-mass PMS stars, known and new high-mass OB stars, and occasionally diffuse X-ray emission from stellar winds or SNRs. In addition to those discussed below, these include NGC 2024 in the Orion B molecular cloud (*Skinner et al.,* 2003), NGC 6193 in Ara OB1 (*Skinner et al.,* 2005), NGC 6334 (*Ezoe et al.,* 2006), NGC 6530 ionizing Messier 8 (*Damiani et al.,* 2004), the Arches and Quintuplet galactic center clusters (*Law and Yusef-Zadeh,* 2004; *Rockefeller et al.,* 2005), and Westerlund 1, which has an X-ray pulsar (*Muno et al.,* 2006; *Skinner et al.,* 2006). Chandra studies of NGC 6357, M 16, RCW 49, W 51A, W 3, and other regions are also underway. Both XMM-Newton and Chandra have examined rich clusters in the Carina Nebula (*Evans et al.,* 2003, 2004; *Albacete Colombo et al.,* 2003), NGC 6231 at the core of the Sco OB1 association, and portions of Cyg OB2.

4.1. Cepheus B, RCW 38, and Stellar Populations

Each Chandra image of a MSFR shows hundreds, sometimes over a thousand, unresolved sources. For regions at distances around $d \simeq 1$–3 kpc, only a small fraction (typically 3–10%) of these sources are background quasars or field galactic stars. The stellar contamination is low because PMS stars are typically 100-fold more X-ray luminous than 1–10-G.y.-old main-sequence stars (Fig. 5a). Since Chandra source positions are accurate to 0.2"–0.4", identifications have little ambiguity except for components of multiple systems. The XLF of a stellar population spans 4 orders of magnitude; 2 orders of magnitude of this range arises from a correlation with stellar mass and bolometric magnitude (*Preibisch et al.,* 2005). This means that the X-ray flux limit of a MSFR observation roughly has a corresponding limit in K-band magnitude and mass. Day-long exposures of regions $d \simeq 2$ kpc away are typically complete to $\log L_x$[erg/s] ~ 29.5, which gives nearly complete samples down to $M \simeq 1\ M_\odot$ with little contamination. We outline two recent studies of this type.

A 27-h Chandra exposure of the stellar cluster illuminating the HII region RCW 38 ($d \simeq 1.7$ kpc) reveals 461 X-ray sources, of which 360 are confirmed cluster members (*Wolk et al.,* 2006). Half have near-infrared counterparts, of which 20% have K-band excesses associated with optically thick disks. The cluster is centrally concentrated with a half-width of 0.2 pc and a central density of 100 X-ray stars/pc^2. Obscuration of the cluster members, seen both in the soft X-ray absorption column and near-infrared photometry, is typically $10 < A_V < 20$ mag. The X-ray stars are mostly unstudied; particular noteworthy are 31 X-ray stars that may be new obscured OB stars. Assuming a standard IMF, the total cluster membership is estimated to exceed 2000 stars. About 15% of the X-ray sources are variable, and several show plasma temperatures exceeding 100 MK.

A recent Chandra study was made of the Sharpless 155 HII region on the interface where stars from the Cep OB3b association ($d = 725$ pc) illuminates the Cepheus B molecular cloud core (*Getman et al.,* 2006a). Earlier, a few ultracompact HII regions inside the cloud indicated an embedded cluster is present, but little was known about the embedded population. The 8-h exposure shows 431 X-ray sources,

of which 89% are identified with K-band stars. Sixty-four highly absorbed X-ray stars inside the cloud provide the best census of the embedded cluster, while the 321 X-ray stars outside the cloud provide the best census of this portion of the Cep OB3b cluster. Surprisingly, the XLF of the unobscured sample has a different shape from that seen in the Orion Nebula Cluster, with an excess of stars around log L_x[erg/s] ≃ 29.7 or M ≃ 0.3 $M_\odot$. It is not clear whether this arises from a deviation in the IMF or some other cause, such as sequential star formation generating a noncoeval population. The diffuse X-rays in this region, which has only one known O star, are entirely attributable to the integrated contribution of fainter PMS stars.

4.2. M 17 and X-Ray Flows in HII Regions

For OB stars excavating an HII region within their nascent molecular cloud, diffuse X-rays may be generated as fast winds shock the surrounding media (*Weaver et al.,* 1977). Chandra has clearly discriminated this diffuse emission from the hundreds of X-ray-emitting young stars in M 17 and the Rosette Nebula (*Townsley et al.,* 2003).

Perhaps the clearest example of diffuse X-ray emission in MSFRs is the Chandra observation of M 17, a bright blownout blister HII region on the edge of a massive molecular cloud (d ≃ 1.6 kpc). The expansion of the blister HII region is triggering star formation in its associated giant molecular cloud, which contains an ultracompact HII region, water masers, and the dense core M 17SW. M 17 has 100 stars earlier than B9 (for comparison, the Orion Nebula Cluster has 8), with 14 O stars. The Chandra image is shown in Plate 3, along with an earlier, wider-field image from the ROSAT satellite. Over 900 point sources in the ~172 × 172 field are found (Broos et al., in preparation).

The diffuse emission of M 17 is spatially concentrated eastward of the stellar cluster and fills the region delineated by the photodissociation region and the molecular cloud. The X-ray spectrum can be modeled as a two-temperature plasma with T = 1.5 MK and 7 MK, and a total intrinsic X-ray luminosity (corrected for absorption) of $L_{x,diffuse} = 3 \times 10^{33}$ erg/s (*Townsley et al.,* 2003). The X-ray plasma has mass M ~ 0.1 $M_\odot$ and density 0.1–0.3 cm^{-3} spread over several cubic parsecs. It represents only ~10^4 yr of recent O-wind production; past wind material has already flowed eastward into the galactic interstellar medium.

The diffuse emission produced by the M 17 cluster, and similar but less dramatic emission by the Rosette Nebula cluster, gives new insight into HII region physics. The traditional HII region model developed decades ago by Strömgren and others omitted the role of OB winds, which were not discovered until the 1960s. The winds play a small role in the overall energetics of HII regions, but they dominate the momentum and dynamics of the nebula with $\frac{1}{2}\dot{M}v_w^2$ ~ $10^{36–37}$ erg/s for a typical early-O star. If completely surrounded by a cold cloud medium, an O star should create a "wind-swept bubble" with concentric zones: a freely expanding wind, a wind termination shock followed by an X-ray emitting zone, the standard T = 10^4 K HII region, the ionization front, and the interface with the cold interstellar environment (*Weaver et al.,* 1977; *Capriotti and Kozminski,* 2001).

These early models predicted L_x ~ 10^{35} erg/s from a single embedded O star, 2 orders of magnitude brighter than the emission produced by M 17 (*Dunne et al.,* 2003). Several explanations for this discrepancy can be envisioned: Perhaps the wind energy is dissipated in a turbulent mixing layer (*Kahn and Breitschwerdt,* 1990), or the wind terminal shock may be weakened by mass-loading of interstellar material (e.g., *Pittard et al.,* 2001). Winds from several OB stars may collide and shock before they hit the ambient medium (*Cantó et al.,* 2000). Finally, a simple explanation may be that most of the kinetic energy of the O star winds remains in a bulk kinetic flow into the galactic interstellar medium (*Townsley et al.,* 2003).

4.3. Trumpler 14 in the Carina Nebula

The Carina complex at d ≃ 2.8 kpc is a remarkably rich star-forming region containing 8 open clusters with at least 64 O stars, several WR stars, and the luminous blue variable η Car. The presence of WR stars may indicate past supernovae, although no well-defined remnant has been identified. One of these clusters is Tr 14, an extremely rich, young (~1 m.y.), compact OB association with ~30 previously identified OB stars. Together with the nearby Trumpler 16 cluster, it has the highest concentration of O3 stars known in the galaxy. Over 20 years ago, an Einstein Observatory X-ray study of the Carina star-forming complex detected a few dozen high-mass stars and diffuse emission attributed to O-star winds (*Seward and Chlebowski,* 1982). Chandra studies show that thousands of the lower-mass stars in these young clusters were likely to be contributing to this diffuse flux; a major goal is to determine the relative contributions of stars, winds, and SNRs to the extended emission in the Carina Nebula.

Plate 4a shows a 16-h Chandra exposure centered on HD 93129AB, the O2I/O3.5V binary at the center of Tr 14 (Townsley et al., in preparation). Over 1600 members of the Tr 14 and Tr 16 clusters can be identified from the X-ray point sources and extensive diffuse emission is clearly present. The diffuse emission surrounding Tr 14 is quite soft with subsolar elemental abundances, similar to the M 17 OB-wind shocks. But the much brighter diffuse emission seen far from the massive stellar clusters is less absorbed and requires enhanced abundances of Ne and Fe. This supports models involving old "cavity" supernova remnants that exploded inside the Carina superbubble (e.g., *Chu et al.,* 1993).

Chandra resolves the two components of HD 93129AB separated by ~3": HD 93129B shows a typical O-star soft X-ray spectrum (T ~ 6 MK), while HD 93129A shows a similar soft component plus a T ~ 35 MK component that dominates the total X-ray luminosity. This hard spectrum and high X-ray luminosity are indicative of a colliding-wind

binary (*Pittard et al.,* 2001), in agreement with the recent finding that HD 93129A is itself a binary (*Nelan et al.,* 2004). Other colliding wind binaries are similarly identified in the cluster.

4.4. The Starburst of 30 Doradus

Plate 4b shows a 6-h Chandra exposure of 30 Dor in the Large Magellanic Cloud, the most luminous giant extragalactic HII region and "starburst cluster" in the Local Group. 30 Dor is the product of multiple epochs of star formation, which have produced multiple SNRs seen with ROSAT as elongated plasma-filled superbubbles on ~100-pc scales (*Wang and Helfand,* 1991).

The new Chandra image shows a bright concentration of X-rays associated with the R136 star cluster, the bright SNR N157B to the southwest, a number of new widely distributed compact X-ray sources, and diffuse structures that fill the superbubbles produced by the collective effects of massive stellar winds and their past supernova events (*Townsley et al.,* 2006a). Some of these are center-filled while others are edge-brightened, indicating a complicated mix of viewing angles and perhaps filling factors. Comparison of the morphologies of the diffuse X-ray emission with the photodissociation region revealed by Hα imaging and cool dust revealed by infrared imaging with the Spitzer Space Telescope shows a remarkable association: The hot plasma clearly fills the cavities outlined by ionized gas and warm dust. Spectral analysis of the superbubbles reveals a range of absorptions (A_V = 1–3 mag), plasma temperatures (T = 3–9 MK), and abundances. About 100 X-ray sources are associated with the central massive cluster R136 (*Townsley et al.,* 2006b). Some are bright, hard X-ray point sources in the field likely to be colliding-wind binaries, while others are probably from ordinary O and WR stellar winds.

5. X-RAY EFFECTS ON STAR AND PLANET FORMATION

5.1. X-Ray Ionization of Molecular Cloud Cores

One of the mysteries of galactic astrophysics is why most interstellar molecular material is not engaged in star formation. Large volumes of most molecular clouds are inactive, and some clouds appear to be completely quiescent. A possible explanation is that star formation is suppressed by ionization: Stellar ultraviolet will ionize the outer edges of clouds, and galactic cosmic rays may penetrate into their cores (*Stahler and Palla,* 2005). Even very low levels of ionization will couple the mostly neutral gas to magnetic fields, inhibiting gravitational collapse until sufficient ambipolar diffusion occurs.

The X-ray observations of star-forming regions demonstrate that a third source of ionization must be considered: X-rays from the winds and flares of deeply embedded X-ray sources. The X-ray ionization zones, sometimes called X-ray dissociation regions (XDRs) or Röntgen spheres, do not have sharp edges like ultraviolet Strömgren spheres, but rather extend to large distances with decreasing effect (*Hollenbach and Tielens,* 1997).

The COUP observation provides a unique opportunity to calculate realistic XDRs in two molecular cloud cores: OMC-1 or the Becklin-Neugebauer region, and OMC-1 South. Several dozen embedded X-ray stars are seen in these clouds (Plate 1), and each can be characterized by X-ray luminosity, spectrum, and line-of-sight absorption (*Grosso et al.,* 2005). Figure 6 illustrates the X-ray properties of deeply embedded objects. COUP #554 is a young star with a strong infrared-excess in the OMC-1 South core. The Chandra spectrum shows soft X-ray absorption of $\log N_H[cm^{-2}] = 22.7$, equivalent to $A_V \sim 30$ mag, and the light-curve exhibits many powerful flares at the top of the XLF with peak X-ray luminosities reaching $\sim 10^{32}$ erg/s. COUP #632 has no optical or K-band counterpart and its X-ray spectrum shows the strongest absorption of all COUP sources: $\log N_H[cm^{-2}] \simeq 23.9$ or $A_V \sim 500$ mag.

Using the COUP source positions and absorptions, we can roughly place each star into a simplified geometrical model of the molecular cloud gas, and calculate the region around each where the X-ray ionization exceeds the expected uniform cosmic-ray ionization. Plate 2 shows the resulting XDRs in OMC-1 from the embedded Becklin-Neugebauer cluster (Lorenzani et al., in preparation). Here a significant fraction of the volume is dominated by X-ray ionization. In general, the ionization of cloud cores ≃0.1 pc in size will be significantly altered if they contain clusters with more than ~50 members.

5.2. X-Ray Irradiation of Protoplanetary Disks

The circumstellar disks around PMS stars where planetary systems form were generally considered to consist of cool, neutral molecular material in thermodynamic equilibrium with ~100–1000 K temperatures. But there is a growing understanding that they are not closed and isolated structures. A few years ago, discussion concentrated on ultraviolet radiation from O stars that can photoevaporate nearby disks (*Hollenbach et al.,* 2000). More recently, considerable theoretical discussion has focused on X-ray irradiation from the host star (Fig. 7). This is a rapidly evolving field and only a fraction of the studies can be mentioned here. Readers are referred to reviews by *Feigelson* (2005) and *Glassgold et al.* (2005) for more detail.

X-ray studies provide two lines of empirical evidence that the X-rays seen with our telescopes actually do efficiently irradiate protoplanetary disks. First, the 6.4-keV fluorescent line of neutral iron is seen in several embedded COUP stars with massive disks, as shown in Fig. 2 (*Imanishi et al.,* 2001). This line is only produced when hard X-rays illuminate >1 g/cm^2 of material; this is too great to be intervening material and must be reflection off of a flattened structure surrounding the X-ray source (*Tsujimoto et al.,* 2005; *Favata et al.,* 2005b). Second, X-ray spectra of PMS stars with inclined disks show more absorption than

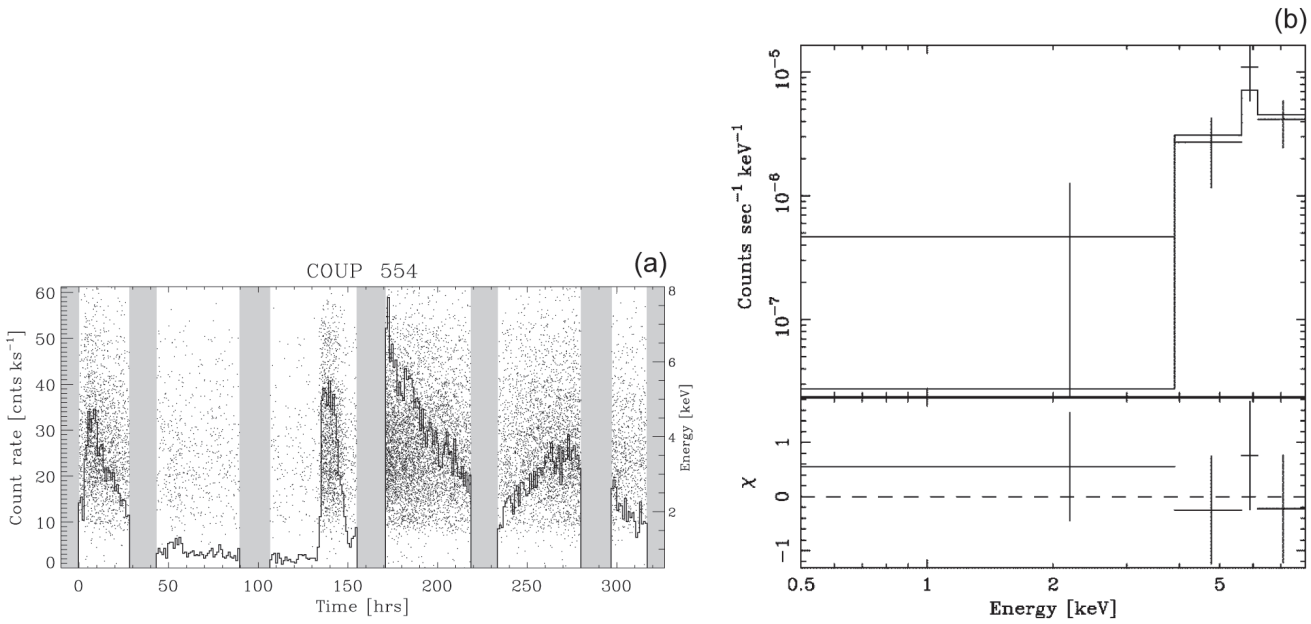

Fig. 6. X-ray properties of two stars deeply embedded in the OMC-1 South molecular cloud core from the Chandra Orion Ultradeep Project. **(a)** Lightcurve of COUP #554 over 13.2 d where the histogram shows the integrated brightness (lefthand vertical axis) and the dots show the energies of individual photons (righthand vertical axis). **(b)** Spectrum of COUP #632 showing very strong absorption at energies below 4 keV. From *Grosso et al.* (2005).

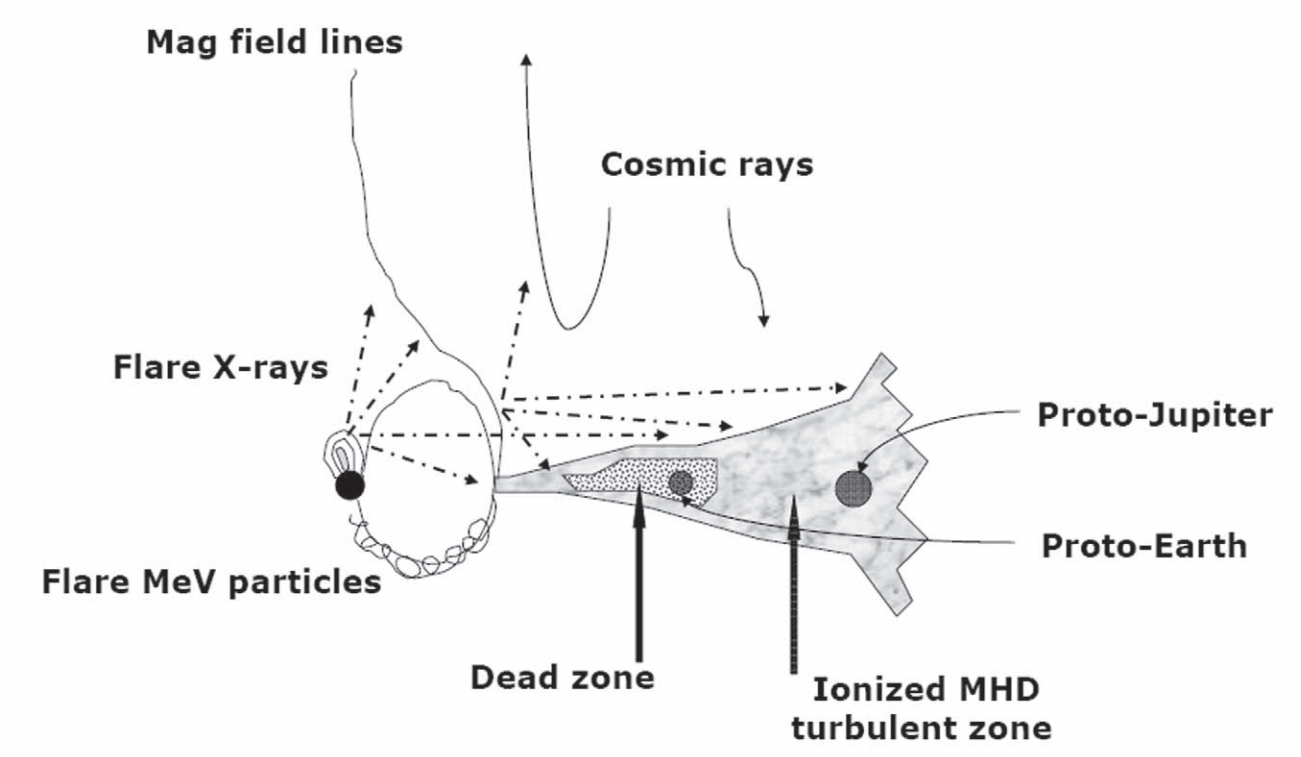

Fig. 7. Cartoon illustrating sources of energetic irradiation (galactic cosmic rays, flare X-rays, flare particles) and their possible effects on protoplanetary disks (ionization of gas and induction of MHD turbulence, layered accretion structure, spallation of solids). From *Feigelson* (2005).

spectra from stars with face-on disks. This is most clearly seen in the COUP survey, where column densities log $N_H[cm^{-2}] \sim 23$ are seen in edge-on proplyds imaged with the Hubble Space Telescope (*Kastner et al.,* 2005). This demonstrates the deposition of ionizing radiation in the disk and gives a rare measurement of the gas (rather than dust) content of protoplanetary disks.

Having established that X-ray emission, particularly X-ray flaring, is ubiquitous in PMS stars, and that at least some disks are efficiently irradiated by these X-rays, one can now estimate the X-ray ionization rate throughout a disk. The result is that X-rays penetrate deeply toward the midplane in the jovian planet region, but leave a neutral "dead zone" in the terrestrial planet region (e.g., *Igea and Glassgold,* 1999; *Fromang et al.,* 2002). The ionization effect of X-rays is many orders of magnitude more important than that of cosmic rays. However, differing treatments of metal ions and dust leads to considerable differences in the inferred steady-state ionization level of the disk (*Ilgner and Nelson,* 2006). The theory of the X-ray ionization *rate* thus appears satisfactory, but calculations of the X-ray ionization *fraction* depend on poorly established recombination rates.

X-ray ionization effects become important contributors to the complex and nonlinear interplay between the thermodynamics, dynamics, gas-phase chemistry, and gas-grain interactions in protoplanetary disks. One important consequence may be the induction of the magnetorotational instability, which quickly develops into a full spectrum of MHD turbulence including both vertical and radial mixing. The radial viscosity associated with the active turbulent zone may cause the flow of material from the outer disk into the inner disk, and thereby into the bipolar outflows and onto the protostar. This may solve a long-standing problem in young stellar studies: A completely neutral disk should have negligible viscosity and thus cannot efficiently be an accretion disk. Ionization-induced turbulence should affect planet formation and early evolution in complex ways: suppressing gravitational instabilities, concentrating solids, producing density inhomogeneities that can inhibit Type I migration of protoplanets, diminishing disk gaps involved in Type II migration, and so forth. It is thus possible that X-ray emission plays an important role in regulating the structure and dynamics of planetary systems, and the wide range in X-ray luminosities may be relevant to the diversity of extrasolar planetary systems.

PMS X-rays are also a major source of ionization at the base of outflows from protostellar disks that produce the emission line Herbig-Haro objects and molecular bipolar outflows (*Shang et al.,* 2002). This is a profound result: If low-mass PMS stars were not magnetically active and profusely emitting penetrating photoionizing radiation, then the coupling between the Keplerian orbits in the disk and the magnetocentrifugal orbits spiralling outward perpendicular to the disks might be much less efficient than we see.

X-ray ionization of a molecular environment will induce a complex series of molecular-ion and radical chemical reactions (e.g., *Aikawa and Herbst,* 1999; *Semenov et al.,* 2004). CN, HCO^+, and C_2H abundances may be good tracers of photoionization effects, although it is often difficult to distinguish X-ray and ultraviolet irradiation from global disk observations. X-ray heating may also lead to ice evaporation and enhanced gaseous abundances of molecules such as methanol. X-ray absorption also contributes to the warming of outer molecular layers of the disk. In the outermost layer, the gas is heated to 5000 K, far above the equilibrium dust temperature (*Glassgold et al.,* 2004). This may be responsible for the strong rovibrational CO and H_2 infrared bands seen from several young disks.

Finally, PMS flaring may address several long-standing characteristics of ancient meteorites that are difficult to explain within the context of a quiescent solar nebula in thermodynamic equilibrium:

1. Meteorites reveal an enormous quantity of flash-melted chondrules. While many explanations have been proposed, often with little empirical support, it is possible that they were melted by the $>10^8$ X-ray flares experienced by a protoplanetary disk during the era of chondrule melting. Melting might either be produced directly by the absorption of X-rays by dustballs (*Shu et al.,* 2001) or by the passage of a shock along the outer disk (*Nakamoto et al.,* 2005).

2. Certain meteoritic components, particularly the calcium-aluminum-rich inclusions (CAIs), exhibit high abundances of daughter nuclides of short-lived radioisotopic anomalies that must have been produced immediately before or during disk formation. Some of these may arise from the injection of recently synthesized radionuclides from supernovae, but other may be produced by spallation from MeV particles associated with the X-ray flares (*Feigelson et al.,* 2002). Radio gyrosynchrotron studies already demonstrate that relativistic particles are frequently present in PMS systems.

3. Some meteoritic grains that were free-floating in the solar nebula show high abundances of spallogenic ^{21}Ne excesses correlated with energetic particle track densities (*Woolum and Hohenberg,* 1993). The only reasonable explanation is irradiation by high fluences of MeV particles from early solar flares.

We thus find that X-ray astronomical studies of PMS stars have a wide variety of potentially powerful effects on the physics, chemistry, and mineralogy of protoplanetary disks and the environment of planet formation. These investigations are still in early stages, and it is quite possible that some of these proposed effects may prove to be uninteresting while others prove to be important.

6. SUMMARY

The fundamental result of X-ray studies of young stars and star-formation regions is that material with characteristic energies of keV (or even MeV) per particle is present in environments where the equilibrium energies of the bulk material are meV. Magnetic reconnection flares in lower-mass PMS stars, and wind shocks on different scales in

O stars, produce these hot gases. Although the X-ray luminosities are relatively small, the radiation effectively penetrates and ionizes otherwise neutral molecular gases and may even melt solids. X-rays from PMS stars may thus have profound effects on the astrophysics of star and planet formation.

The recent investigations outlined here from the Chandra and XMM-Newton observatories paint a rich picture of X-ray emission in young stars. Both the ensemble statistics and the characteristics of individual X-ray flares strongly resemble the flaring seen in the Sun and other magnetically active stars. Astrophysical models of flare cooling developed for solar flares fit many PMS flares well. PMS spectra show the same abundance anomalies seen in older stars. Rotationally modulated X-ray variability of the nonflaring characteristic emission show that the X-ray emitting structures lie close to the stellar surface and are inhomogeneously distributed in longitude. This is a solid indication that the X-ray emitting structures responsible for the observed modulation are in most cases multipolar magnetic fields, as on the Sun.

At the same time, the analysis of the most powerful flares indicates that very long magnetic structures are likely present in some of the most active PMS stars, quite possibly connecting the star with its surrounding accretion disk. The evidence suggests that both coronal-type and star-disk magnetic field lines are present in PMS systems, in agreement with current theoretical models of magnetically funnelled accretion.

There is a controversy over the X-ray spectra of a few of the brightest accreting PMS stars. TW Hya shows low plasma temperatures and emission lines, suggesting an origin in accretion shocks rather than coronal loops. However, it is a challenge to explain the elemental abundances and to exclude the role of ultraviolet irradiation. Simultaneous optical observations during the COUP X-ray observation clearly shows that the bulk of X-ray emission does not arise from accretion processes. Perhaps counterintuitively, various studies clearly show that accreting PMS stars are statistically weaker X-ray emitters than nonaccretors. A fraction of the magnetic field lines in accreting PMS stars are likely to be mass loaded and cannot reach X-ray temperatures.

X-ray images of high-mass star-forming regions are incredibly rich and complex. Each image shows hundreds or thousands of magnetically active PMS stars with ages ranging from Class I (and controversially, Class 0) protostars to zero-age main-sequence stars. Hard X-rays are often emitted so that Chandra can penetrate up to $A_V \simeq 500$ mag into molecular cloud material. Chandra images of MSFRs also clearly reveal for the first time the fate of O-star winds: The interiors of some HII regions are suffused with a diffuse 10 MK plasma, restricting the 10^4 K gas to a thin shell. The concept of a Strömgren sphere must be revised in these cases. Only a small portion of the wind energy and mass appears in the diffuse X-ray plasma; most likely flows unimpeded into the galactic interstellar medium. The full population of stars down to ~1 $M_\odot$ is readily seen in X-ray images of MSFRs, with little contamination from extraneous populations. This may lead, for example, to X-ray-based discrimination of close OB binaries with colliding winds and identification of intermediate-mass PMS stars that are not accreting. In the most active and long-lived MSFRs, cavity SNRs and superbubbles coexist with, and may dominate, the stellar and wind X-ray components. X-ray studies thus chronicle the life cycle of massive stars from proto-O stars to colliding O winds, to supernova remnants and superbubbles. These star-forming regions represent the building blocks of galactic-scale star formation and starburst galaxies.

Some of the issues discussed here are now well developed while others are still in early stages of investigation. It is unlikely that foreseeable studies will give qualitatively new information on the X-ray properties of low-mass PMS stars than obtained from the many studies emerging from the COUP and XEST projects. In-depth analysis of individual objects, especially high-resolution spectroscopic study, represents an important area ripe for follow-up exploration. The many X-ray studies of MSFRs now emerging should give large new samples of intermediate-mass stars, and new insights into the complex physics of OB stellar winds on both small and large scales. Although Chandra and XMM-Newton have relatively small fields, a commitment to wide-field mosaics of MSFR complexes like W3-W4-W5 and Carina could give unique views into the interactions of high-mass stars and the galactic interstellar medium. Deep X-ray exposures are needed to penetrate deeply to study the youngest embedded systems. Finally, the next generation of high-throughput X-ray telescopes should bring new capabilities to perform high-resolution spectroscopy of the X-ray emitting plasmas. Today, theoretical work is urgently needed on a host of issues raised by the X-ray findings: magnetic dynamos in convective stars, accretion and reconnection in disk-star magnetic fields, flare physics at levels far above those seen in the Sun, and possible effects of X-ray ionization of protoplanetary disks.

Acknowledgments. E.D.F. recognizes the excellent work by K. Getman and the other 36 scientists in the COUP collaboration. E.D.F. and L.K.T. benefit from discussions with their Penn State colleagues P. Broos, G. Garmire, K. Getman, M. Tsujimoto, and J. Wang. Penn State work is supported by the National Aeronautics and Space Administration (NASA) through contract NAS8-38252 and Chandra Awards G04-5006X, G05-6143X, and SV4-74018 issued by the Chandra X-ray Observatory Center, operated by the Smithsonian Astrophysical Observatory for and on behalf of NASA under contract NAS8-03060. M.G. warmly acknowledges the extensive work performed by XEST team members. The XEST team has been financially supported by the Space Science Institute (ISSI) in Bern, Switzerland. XMM-Newton is an ESA science mission with instruments and contributions directly funded by ESA Member States and the U.S. (NASA). K.G.S. is grateful for funding support from NSF CAREER grant AST-0349075.

REFERENCES

Aikawa Y. and Herbst E. (1999) *Astron. Astrophys., 351,* 233–246.

Albacete Colombo J. F., Méndez M., and Morrell N. I. (2003) *Mon. Not. R. Astron. Soc., 346,* 704–718.

Arzner K. and Güdel M. (2004) *Astrophys. J., 602,* 363–376.

Audard M., Güdel M., Skinner S. L., Briggs K. R., Walter F. M., et al. (2005) *Astrophys. J., 635,* L81–L84.

Barnes S. A. (2003a) *Astrophys. J., 586,* 464–479.

Barnes S. A. (2003b) *Astrophys. J., 586,* L145–L147.

Brinkman A. C., Behar E., Güdel M., Audard M., den Boggende A. J. F., et al. (2001) *Astron. Astrophys., 365,* L324–L328.

Calvet N., D'Alessio P., Hartmann L., Wilner D., Walsh A., and Sitko M. (2002) *Astrophys. J., 568,* 1008–1016.

Cantó J., Raga A. C., and Rodríguez L. F. (2000) *Astrophys. J., 536,* 896–901.

Capriotti E. R. and Kozminski J. F. (2001) *Publ. Astron. Soc. Pac., 113,* 677–691.

Chu Y.-H., Mac Low M.-M., Garcia-Segura G., Wakker B., and Kennicutt R. C. (1993) *Astrophys. J., 414,* 213–218.

Damiani F., Flaccomio E., Micela G., Sciortino S., Harnden F. R. Jr., and Murray S. S. (2004) *Astrophys. J., 608,* 781–796.

Drake J. J., Testa P., and Hartmann L. (2005) *Astrophys. J., 627,* L149–L152.

Dunne B. C., Chu Y.-H., Chen C.-H. R., Lowry J. D., Townsley L., et al. (2003) *Astrophys. J., 590,* 306–313.

Evans N. R., Seward F. D., Krauss M. I., Isobe T., Nichols J., et al. (2003) *Astrophys. J., 589,* 509–525.

Evans N. R., Schlegel E. M., Waldron W. L., Seward F. D., Krauss M. I., et al. (2004) *Astrophys. J., 612,* 1065–1080.

Ezoe Y., Kokubun M., Makishima K., Sekimoto Y., and Matsuzaki K. (2006) *Astrophys. J., 638,* 860–877.

Favata F. and Micela G. (2003) *Space Sci. Rev., 108,* 577–708.

Favata F., Giardino G., Micela G., Sciortino S., and Damiani F. (2003) *Astron. Astrophys., 403,* 187–203.

Favata F., Flaccomio E., Reale F., Micela G., Sciortino S., et al. (2005a) *Astrophys. J. Suppl., 160,* 469–502.

Favata F., Micela G., Silva B., Sciortino S., and Tsujimoto M. (2005b) *Astron. Astrophys. 433,* 1047–1054.

Feigelson E. D. (2005) In *Proc. 13th Cool Stars Workshop* (F. Favata et al., eds.), pp. 175–183. ESA SP-560, Noordwijk.

Feigelson E. D. and Montmerle T. (1999) *Ann. Rev. Astron. Astrophys., 37,* 363–408.

Feigelson E. D., Garmire G. P., and Pravdo S. H. (2002) *Astrophys. J., 572,* 335–349.

Feigelson E. D., Gaffney J. A., Garmire G., Hillenbrand L. A., and Townsley L. (2003) *Astrophys. J., 584,* 911–930.

Feigelson E. D., Hornschemeier A. E., Micela G., Bauer F. E., Alexander D. M., et al. (2004) *Astrophys. J., 611,* 1107–1120.

Feigelson E. D., Getman K., Townsley L., Garmire G., Preibisch T., et al. (2005) *Astrophys. J. Suppl., 160,* 379–389.

Flaccomio E., Micela G., and Sciortino S. (2003) *Astron. Astrophys., 402,* 277–292.

Flaccomio E., Micela G., Sciortino S., Feigelson E. D., Herbst W., et al. (2005) *Astrophys. J. Suppl., 160,* 450–468.

Fromang S., Terquem C., and Balbus S. A. (2002) *Mon. Not. R. Astron. Soc., 329,* 18–28.

Gagné M., Skinner S. L., and Daniel K. J. (2004) *Astrophys. J., 613,* 393–415.

Getman K. V., Feigelson E. D., Townsley L., Bally J., Lada C. J., and Reipurth B. (2002) *Astrophys. J., 575,* 354–377.

Getman K. V., Flaccomio E., Broos P. S., Grosso N., Tsujimoto M., et al. (2005a) *Astrophys. J. Suppl., 160,* 319–352.

Getman K. V., Feigelson E. D., Grosso N., McCaughrean M. J., Micela G., et al. (2005b) *Astrophys. J. Suppl., 160,* 353–378.

Getman K. V., Feigelson E. D., Townsley L., Broos P., Garmire G., Tsujimoto M. (2006a) *Astrophys. J. Suppl., 163,* 306–334.

Getman K. V., Feigelson E. D., Garmire G., Broos R., and Wang J. (2006b) *Astrophys. J.,* in press.

Glassgold A. E., Feigelson E. D., and Montmerle T. (2000) In *Protostars and Planets IV* (V. Mannings et al., eds.), pp. 429–456. Univ. of Arizona, Tucson.

Glassgold A. E., Najita J., and Igea J. (2004) *Astrophys. J., 615,* 972–990.

Glassgold A. E., Feigelson E. D., Montmerle T., and Wolk S. (2005) In *Chondrites and the Protoplanetary Disk* (A. N. Krot et al., eds.), pp. 161–180. ASP Conf. Series 341, San Francisco.

Grosso N., Montmerle T., Feigelson E. D., and Forbes T. G. (2004) *Astron. Astrophys., 419,* 653–665.

Grosso N., Feigelson E. D., Getman K. V., Townsley L., Broos P., et al. (2005) *Astrophys. J. Suppl., 160,* 530–556.

Grosso N., et al. (2006) *Astron. Astrophys.,* in press.

Güdel M. (2002) *Ann. Rev. Astron. Astrophys., 40,* 217–261.

Güdel M. (2004) *Astron. Astrophys. Rev., 12,* 71–237.

Güdel M., Guinan E. F., and Skinner S. L. (1997) *Astrophys. J., 483,* 947–960.

Güdel M., Audard M., Kashyap V. L., Drake J. J., and Guinan E. F. (2003) *Astrophys. J., 582,* 423–442.

Hamaguchi K., Corcoran M. F., Petre R., White N. E., Stelzer B., et al. (2005) *Astrophys. J., 623,* 291–301.

Hartmann L. (1998) *Accretion Processes in Star Formation,* Cambridge Univ., New York.

Herbst W., Bailer-Jones C. A. L., Mundt R., Meisenheimer K., and Wackermann R. (2002) *Astron. Astrophys., 396,* 513–532.

Hollenbach D. J. and Tielens A. G. G. M. (1997) *Ann. Rev. Astron. Astrophys., 35,* 179–216.

Hollenbach D. J., Yorke H. W., and Johnstone D. (2000) In *Protostars and Planets IV* (V. Mannings et al., eds.), pp. 401–416. Univ. of Arizona, Tucson.

Igea J. and Glassgold A. E. (1999) *Astrophys. J., 518,* 848–858.

Imanishi K., Koyama K., and Tsuboi Y. (2001) *Astrophys. J., 557,* 747–760.

Ilgner M. and Nelson R. P. (2006) *Astron. Astrophys., 445,* 223–232.

Jardine M. and Unruh Y. C. (1999) *Astron. Astrophys., 346,* 883–891.

Jardine M., Collier Cameron A., Donati J.-F., Gregory S. G., and Wood K. (2006) *Mon. Not. R. Astron. Soc., 367,* 917–927.

Johns-Krull C. M., Valenti J. A., and Saar S. H. (2004) *Astrophys. J., 617,* 1204–1215.

Kahn F. D. and Breitschwerdt D. (1990) *Mon. Not. R. Astron. Soc., 242,* 209–214.

Kashyap V. L., Drake J. J., Güdel M., and Audard M. (2002) *Astrophys. J., 580,* 1118–1132.

Kastner J. H., Huenemoerder D. P., Schulz N. S., Canizares C. R., and Weintraub D. A. (2002) *Astrophys. J., 567,* 434–440.

Kastner J. H., Richmond M., Grosso N., Weintraub D. A., Simon T., et al. (2004) *Nature, 430,* 429–431.

Kastner J. H., Franz G., Grosso N., Bally J., McCaughrean M. J., et al. (2005) *Astrophys. J. Suppl., 160,* 511–529.

Lamzin S. A. (1999) *Astron. Lett., 25,* 430–436.

Law C. and Yusef-Zadeh F. (2004) *Astrophys. J., 611,* 858–870.

Loinard L., Mioduszewski A. J., Rodríguez L. F., González R. A., Rodríguez M. I., and Torres R. M. (2005) *Astrophys. J., 619,* L179–L182.

Montmerle T., Grosso N., Tsuboi Y., and Koyama K. (2000) *Astrophys. J., 532,* 1097–1110.

Mullan D. J. and MacDonald J. (2001) *Astrophys. J., 559,* 353–371.

Muno M. P., Clark J. S., Crowther P. A., Dougherty S. M., de Grijs R., et al. (2006) *Astrophys. J., 636,* L41–L44.

Nakamoto T. and Miura H. (2005) In *PPV Poster Proceedings,* www.lpi.usra.edu/meetings/ppv2005/pdf/8530.pdf.

Nelan E. P., Walborn N. R., Wallace D. J., Moffat A. F. J., Makidon R. B., et al. (2004) *Astron. J., 128,* 323–329.

Ness J.-U. and Schmitt J. H. M. M. (2005) *Astron. Astrophys., 444,* L41–L44.

Ness J.-U. and Schmitt J. H. M. M. (2006) *Astron. Astrophys.,* in press.

Nielbock M., Chini R., and Müller S. A. H. (2003) *Astron. Astrophys., 408,* 245–256.

Pace G. and Pasquini L. (2004) *Astron. Astrophys., 426,* 1021–1034.

Paerels F. B. S. and Kahn S. M. (2003) *Ann. Rev. Astron. Astrophys., 41,* 291–342.

Parker E. N. (1998) *Astrophys. J., 330,* 474–479.

Pittard J. M., Hartquist T. W., and Dyson J. E. (2001) *Astron. Astrophys., 373,* 1043–1055.

Preibisch T. (2004) *Astron. Astrophys., 428,* 569–577.

Preibisch T. and Feigelson E. D. (2005) *Astrophys. J. Suppl., 160,* 390–400.

Preibisch T., Neuhäuser R., and Alcalá J. M. (1995) *Astron. Astrophys., 304,* L13–L16.

Preibisch T., Kim Y.-C., Favata F., Feigelson E. D., Flaccomio E., et al. (2005) *Astrophys. J. Suppl., 160,* 401–422.

Priest E. R. and Forbes T. G. (2002) *Astron. Astrophys. Rev., 10,* 313–377.

Rockefeller G., Fryer C. L., Melia F., and Wang Q. D. (2005) *Astrophys. J., 623,* 171–180.

Scelsi L., Maggio A., Peres G., and Pallavicini R. (2005) *Astron. Astrophys., 432,* 671–685.

Schmitt J. H. M. M., Robrade J., Ness J.-U., Favata F., and Stelzer B. (2005) *Astron. Astrophys., 432,* L35–L38.

Schrijver C. J. and Zwaan C. (2000) *Solar and Stellar Magnetic Activity,* Cambridge Univ., New York.

Semenov D., Weibe D., and Henning Th. (2004) *Astron. Astrophys., 417,* 93–106.

Seward F. D. and Chlebowski T. (1982) *Astrophys. J., 256,* 530–542.

Shang H., Glassgold A. E., Shu F. H., and Lizano S. (2002) *Astrophys. J., 564,* 853–876.

Shu F. H., Najita J. R., Shang H., and Li Z.-Y. (2000) In *Protostars and Planets IV* (V. Mannings et al., eds.), pp. 789–814. Univ. of Arizona, Tucson.

Shu F. H., Shang H., Gounelle M., Glassgold A. E., and Lee T. (2001) *Astrophys. J., 548,* 1029–1050.

Siess L., Forestini M., and Bertout C. (1999) *Astron. Astrophys., 342,* 480–491.

Skinner S., Gagné M., and Belzer E. (2003) *Astrophys. J., 598,* 375–391.

Skinner S. L., Zhekov S. A., Palla F., and Barbosa C. L. D. R. (2005) *Mon. Not. R. Astron. Soc., 361,* 191–205.

Skinner S. L., et al. (2006) *Astrophys. J. Lett., 639,* L35–L38.

Skumanich A. (1972) *Astrophys. J., 171,* 565–567.

Stahler S. W. and Palla F. (2005) *The Formation of Stars,* Wiley-VCH, New York.

Stassun K. G., Ardila D. R., Barsony M., Basri G., and Mathieu R. D. (2004) *Astron. J., 127,* 3537–3552.

Stassun K. G., van den Berg M., Feigelson E., and Flaccomio E. (2006) *Astrophys. J.,* in press.

Stelzer B. and Schmitt J. H. M. M. (2004) *Astron. Astrophys., 418,* 687–697.

Swartz D. A., Drake J. J., Elsner R. F., Ghosh K. K., Grady C. A., et al. (2005) *Astrophys. J., 628,* 811–816.

Townsley L. K., Feigelson E. D., Montmerle T., Broos P. S., Chu Y.-H., and Garmire G. P. (2003) *Astrophys. J., 593,* 874–905.

Townsley L. K., Broos P. S., Feigelson E. D., Brandl B. R., Chu Y.-H., Garmire G. P., and Pavlov G. G. (2006a) *Astron. J., 131,* 2140–2163.

Townsley L. K., Broos P. S., Feigelson E. D., Garmire G. P., and Getman K. V. (2006b) *Astron. J., 131,* 2164–2184.

Tsuboi Y., Imanishi K., Koyama K., Grosso N., and Montmerle T. (2000) *Astrophys. J., 532,* 1089–1096.

Tsuboi Y., Koyama K., Hamaguchi K., Tatematsu K., Sekimoto Y., et al. (2001) *Astrophys. J., 554,* 734–741.

Tsujimoto M., Feigelson E. D., Grosso N., Micela G., Tsuboi Y., et al. (2005) *Astrophys. J. Suppl., 160,* 503–510.

Wang Q. and Helfand D. J. (1991) *Astrophys. J., 373,* 497–508.

Weaver R., McCray R., Castor J., Shapiro P., and Moore R. (1977) *Astrophys. J., 218,* 377–395.

Wolk S. J., Harnden F. R. Jr., Flaccomio E., Micela G., Favata F., et al. (2005) *Astrophys. J. Suppl., 160,* 423–449.

Wolk S. J., et al. (2006) *Astrophys. J.,* in press.

Woolum D. S. and Hohenberg C. (1993) In *Protostars and Planets III* (E. H. Levy and J. I. Lunine, eds.), pp. 903–919. Univ. of Arizona, Tucson.